

# Salivary Gland Mucosa-Associated Lymphoid Tissue–Type Lymphoma From Sjögren’s Syndrome Patients in the Majority Express Rheumatoid Factors Affinity-Selected for IgG

Richard J. Bende,<sup>1</sup>  Jerry Janssen,<sup>1</sup>  Anna Beentjes,<sup>1</sup>  Thera A. M. Wormhoudt,<sup>1</sup> Koen Wagner,<sup>2</sup>   
Erlin A. Haacke,<sup>3</sup> Frans G. M. Kroese,<sup>3</sup> Jeroen E. J. Guikema,<sup>1</sup>  and Carel J. M. van Noesel<sup>1</sup> 

**Objective.** Patients with Sjögren’s syndrome (SS) have an increased risk of developing malignant B cell lymphomas, particularly mucosa-associated lymphoid tissue (MALT)–type lymphomas. We have previously shown that a predominant proportion of patients with SS-associated salivary gland MALT lymphoma express somatically hypermutated IgM with strong amino acid sequence homology with stereotypic rheumatoid factors (RFs). The present study was undertaken in a larger cohort of patients with SS-associated MALT lymphoma to more firmly assess the frequency of RF reactivity and the significance of somatic *IGV*-region mutations for RF reactivity.

**Methods.** B cell antigen receptors (BCRs) of 16 patients with SS-associated salivary gland MALT lymphoma were analyzed. Soluble recombinant IgM was produced of 12 MALT lymphoma samples, including 1 MALT lymphoma sample that expressed an IgM antibody fitting in a novel *IGHV3-30*–encoded stereotypic *IGHV* subset. For 4 of the 12 IgM antibodies from MALT lymphoma samples, the somatically mutated *IGHV* and *IGKV* gene sequences were reverted to germline configurations. Their RF activity and binding affinity were determined by enzyme-linked immunosorbent assay and surface plasmon resonance, respectively.

**Results.** Nine (75%) of the 12 IgM antibodies identified in patients with SS-associated salivary gland MALT lymphoma displayed strong monoreactive RF activity. Reversion of the *IGHV* and *IGKV* mutations to germline configuration resulted in RF affinities for IgG that were significantly lower for 3 of the 4 somatically mutated IgM antibodies. In stereotypic *IGHV3-7/IGKV3-15*–encoded RFs, a recurrent replacement mutation in the *IGKV3-15*–third complementarity-determining region was found to play a pivotal role in the affinity for IgG-Fc.

**Conclusion.** A majority of patients with SS-associated salivary gland MALT lymphoma express somatically mutated BCRs that are selected for monoreactive, high-affinity binding of IgG-Fc. These data underscore the notion that soluble IgG, most likely in immune complexes in inflamed tissues, is the principal autoantigen in the pathogenesis of a variety of B cell lymphomas, particularly SS-associated MALT lymphomas.

## INTRODUCTION

Mucosa-associated lymphoid tissue (MALT)–type lymphomas account for 5–10% of all B cell lymphomas. These lymphomas occur at various anatomic sites affected by chronic inflammation emerging from pathogens or autoimmunity (1–4). Among all auto-immune diseases, Sjögren’s syndrome (SS) is most strongly associated with lymphoma development, in particular salivary gland MALT lymphomas (1–7). Clinical predictors of lymphoma development

are swelling of the salivary glands, splenomegaly, lymphadenopathy, and palpable purpura. The main biologic predictors are cryoglobulinemia, lymphopenia, low complement levels, and a monoclonal component in the serum or urine (3,4). Recently, the presence of rheumatoid factors (RFs) in the serum was identified as an independent predictor of lymphoma development (8).

Previously, we have shown that ~40% of patients with salivary gland MALT lymphoma express near-identical (also called stereotypic) B cell antigen receptors (BCRs), with a striking degree

Supported by the Dutch Arthritis Foundation (grant 15-2-310) and the Dutch Cancer Society (grant UVA 2014-6824).

<sup>1</sup>Richard J. Bende, PhD, Jerry Janssen, MSc, Anna Beentjes, BSc, Thera A. M. Wormhoudt, BSc, Jeroen E. J. Guikema, PhD, Carel J. M. van Noesel, MD, PhD: Amsterdam University Medical Center and University of Amsterdam, Amsterdam, The Netherlands; <sup>2</sup>Koen Wagner, PhD: AIMM Therapeutics, Amsterdam, The Netherlands; <sup>3</sup>Erlin A. Haacke, MD, MSc, Frans G. M. Kroese, PhD: University Medical Center Groningen and University of Groningen, Groningen, The Netherlands.

No potential conflicts of interest relevant to this article were reported.

Address correspondence to Richard J. Bende, PhD, Amsterdam University Medical Center, Department of Pathology, Meibergdreef 9, 1105 AZ Amsterdam, The Netherlands. Email: r.j.bende@amsterdamumc.nl.

Submitted for publication October 2, 2019; accepted in revised form March 12, 2020.

of VH-third complementarity-determining region (CDR3) amino acid (aa) sequence homology with stereotypic RFs (9). Five groups of stereotypic RFs, each characterized by a canonical combination of *IGHV* and *IGKV* gene sequences and a distinct VH-CDR3, have been identified. They are encoded by 2 distinct *IGHV1-69/JH4* rearrangements, designated as V1-69-RF and WOL-RF (also known as RFs of the Wa idotype), and by *IGHV3-7/JH3*, *IGHV4-59/JH2*, and *IGHV4-59/JH5* rearrangements, designated V3-7-RF, V4-59-RF, and V4-59/JH5-RF, respectively (9,10). Stereotypic RF BCRs are also frequently expressed in gastric MALT lymphoma and hepatitis C virus (HCV)-related B cell lymphoma, and less frequently in ocular adnexal MALT lymphoma, splenic marginal zone B cell lymphoma, diffuse large B cell lymphoma, and B cell chronic lymphocytic leukemia (CLL) (9–15). Polyclonal stereotypic RFs are frequently present in HCV-infected patients with type II mixed cryoglobulinemia and in donors immunized with mismatched red blood cells (16,17).

In a previous study by our group (9) and by Martin et al (18), soluble IgM antibodies were recombinantly produced from SS-associated salivary gland MALT lymphomas of a total of 8 patients, 6 of which showed strong monoreactive RF activity. Two of these 6 RFs were encoded by stereotypic RF *IGHV* rearrangements, i.e., V1-69-RF and V3-7-RF, respectively. Interestingly, all of the RFs expressed either an *IGKV3-15*-encoded or *IGKV3-20*-encoded light chain, both of which are also typically expressed by *IGHV3-7*-encoded and *IGHV1-69*-encoded stereotypic RFs.

In the present study, we assessed the configuration and specificity of the BCRs of 16 patients with SS-associated salivary gland MALT lymphoma, and examined the contribution of the somatic mutations present in *IGHV* and *IGKV* on the affinity of RFs for IgG-Fc.

## PATIENTS AND METHODS

**MALT lymphoma tissue samples.** Frozen salivary gland tissue samples from patients with SS-associated MALT lymphoma (patient samples M83, M86–M89, M91, and M93–M96) were obtained from the Departments of Pathology, Rheumatology, and Clinical Immunology at University Medical Center Groningen, The Netherlands. In addition, paraffin-embedded salivary gland tissue from 1 patient (sample M83) was obtained from the Department of Pathology at Haaglanden Medical Center, The Hague, The Netherlands. The salivary gland samples from patients M5, M8, M11, M14, M21, and M22 have been described previously (9). Available serologic data from patients M86–M89, M91, and M93–M96 showed that all were positive for IgM-RF, anti-SSA, and, except for patients M87 and M91, anti-SSB antibodies. Patients M91, M93, and M94 had low serum C4 levels (the patients' immunohistochemical and serologic data are provided in Supplementary Table 1, available on the *Arthritis & Rheumatology* web site at <http://onlinelibrary.wiley.com/doi/10.1002/art.41263/abstract>).

Presence of IgM-RF and low levels of C4 are biologic predictors of lymphoma development (3,4,8).

The study was conducted in accordance with the ethics standards of our institutional medical ethics committee on human experimentation, as well as in accordance with the 1975 Declaration of Helsinki, as revised in 1983.

**Immunoglobulin gene analysis.** Of the salivary gland tissue from patients with SS-associated MALT lymphoma, Ig clonality was assessed by polymerase chain reaction (PCR). In addition, immunohistochemical analyses were used to detect light-chain restriction in those MALT lymphoma salivary gland samples showing plasmacytic differentiation, with monotypic IgM $\kappa$  expression observed in 10 samples (M5, M8, M11, M21, M83, M86, M91, M93, M94, and M95), and IgA $\kappa$  expression in 2 samples (M14 and M22). Salivary gland tissue from patient M96 expressed IgM, but immunohistochemical staining for the  $\kappa$  and  $\lambda$  light chains was indeterminate. In the samples from patients M87, M88, and M89, immunohistochemical staining for both the Ig heavy chain and Ig light chain was indeterminate (see Supplementary Table 1 [<http://onlinelibrary.wiley.com/doi/10.1002/art.41263/abstract>]). However, in analyses by reverse transcription-PCR (RT-PCR) aimed at IgM, IgG, and IgA transcripts, it was found that the salivary gland tissue from patients M87, M88, and M89 expressed monoclonal IgM (Table 1).

In the paraffin-embedded salivary gland tissue obtained from patient M83, DNA was isolated using a QIAamp DNA Mini kit (Qiagen). RNA from all other MALT lymphoma salivary gland samples was isolated using TRI Reagent (Sigma-Aldrich, Merck), and complementary DNA was synthesized using Pd(N)6 random primers and Moloney murine virus RT (Invitrogen, Fisher Scientific), according to the manufacturer's protocol. The rearranged *IGHV* genes were amplified using *IGHV* primers specific for the framework region 1 (FR1) and FR2, in combination with fluorochrome-labeled reverse primers specific for Ig J $\mu$  and the constant regions of IgM (C $\mu$ ), IgG (C $\gamma$ ), and IgA (C $\alpha$ ) (19). The *IGHV* PCR products were analyzed by gene scanning (VH-CDR3 spectratyping). In salivary gland samples M86–M89, M91, and M93–M96, the FR1/FR2 PCR products with the C $\mu$  primer yielded clonal *IGHV* PCR products. In the salivary gland tissue from patient M93, 2 clonal peaks were detected. The FR1/FR2 PCR with the C $\gamma$  primer yielded polyclonal *IGHV* PCR products in all MALT lymphoma samples. The FR1/FR2 PCR C $\alpha$  primer yielded polyclonal or oligoclonal *IGHV* PCR products in most of the MALT lymphoma samples. An FR1/FR2 PCR with the Ig J $\mu$  downstream primer was performed on the DNA sample from patient M83, which resulted in an *IGHV* PCR product with a monoclonal component. The clonal *IGHV* PCR products were sequenced using a Big Dye Terminator sequencing kit (ThermoFisher Scientific). The *IGHV* sequences were analyzed using V-Quest on the IMGT web site (<http://www.imgt.org/>) (20). *IGKV* PCR was performed with *IGKV* family-specific leader primers, combined with either Ig J $\kappa$  or Ig J $\kappa$ -constant region primers.

**Table 1.** *IGHV* and *IGKV* sequences of 10 salivary gland mucosa-associated lymphoid tissue-type lymphomas of Sjögren's syndrome patients

Patient	Ig isotype*	<i>IGHV</i> ; <i>IGKV</i> rearrangements	<i>IGHV</i> ; <i>IGKV</i> somatic mutation†	VH-CDR3; VK-CDR3 sequence‡	VH-CDR3; VK-CDR3 length§	IgM produced
M83	IgM	V3-74/D4-23/JH4; VK1-39/JK1	22; 9	C AREYGNRFFDY WGQG; C QQSYTSPT FGQG	12; 9	No
M86	IgM	V3-30/D6-13/JH4; VK3-15/JK1	21; 11	C AQQAFSNKWYSIGDY WGQG; C QQYNNWPPWT FGQG	15; 10	Yes
M87	IgM	V1-2/D5-18/JH5	17	C ARGQGTQVSHSWFDP WGQG	15	No
M88	IgM	V1-69/D5-12/JH4	21	C AREGKASVANGAFDY WGQG	15	No
M89	IgM	V4-59/D6-6/JH3; VK3-15/JK1	5; 5/7	C ARDIANIATRRDDAFDI WGQG; C QHYNNWPPWT FGQG	17; 10	Yes
M91	IgM	V1-69/D5-24/JH4; VK3-20/JK2	7; 0	C ARKGDDRDAYDVFY WGQG; C QQYGGSSPYT FGQG	16; 9	Yes
M93-I	IgM	V3-7/D3-22/JH3; VK3-15/JK1	6/9; 5	C ARGDYDSSGGS(S/N)YHDAFDV WGQG; C QHYNNWPPWT FGQG	19; 10	Yes
M93-II	IgM	V4-59/D3-10/JH5; VK4-1/JK2	12; 11	C ACGGGSGTYFRGWFD WGQG; C QQYSTLYT FGQG	17; 9	No
M94	IgM	V3-7/D3-22/JH3; VK3-15/JK1	10; 5	C ARGDYDSSGGYIDAFDI WGQG; C QHYNNWPPWT FGQG	18; 10	Yes
M95	IgM	V3-48/D3-22/JH3; VK3-15/JK4	18; 12	C AREPYSDSSFFPGSFDI WGQG; C QQYDNWPLT FGGG	18; 9	No
M96	IgM	V3-30.3/D2-8/JH3; VK3D-15/JK1	23/24; 4	C ARAGQGSNGIW(G/D) GAFD(T/S) WGQG; C QHYNNWPPWT FGQG	17; 10	Yes

\* Determined by reverse transcription–polymerase chain reaction.

† Values are the number of mutations. Two values separated by a slash sign signify identification of molecular *IGHV/IGKV* clones harboring slightly different numbers of somatic mutations.

‡ For the VH- and VK-third complementarity-determining region (CDR3) sequences in which 2 amino acids separated by a slash sign are depicted, this indicates that 2 molecular *IGHV* clones with dissimilar amino acids at this position were identified.

§ Values are the number of amino acids.

The *IGKV* sequences were analyzed using V-Quest on the IMGT web site.

**Production of recombinant MALT lymphoma-derived IgM antibodies.** The *IGHV* sequences obtained using the FR1 × C<sub>μ</sub> PCR products and appropriate *IGHV* family-specific leader primers, combined with an Ig J<sub>H</sub> primer, were used to produce full-length *IGHV* gene products. The full-length *IGHV* PCR products were obtained as described above. The complete *IGHV* and *IGKV* genes were cloned in pTOPO-TA plasmids and subsequently in the pIGH(μ) and pIGL(κ) expression plasmids, which were then cotransfected in SP2/0 myeloma cells, as previously described (9). Supernatants of the transfected SP2/0 cells were screened for IgMk production, using enzyme-linked immunosorbent assays (ELISAs). The various *IGHV* and *IGKV* full-length sequences in which somatic mutations were reverted to germline configuration (as seen in salivary gland samples M91, M93, M94, and M96) were ordered from GenScript.

**Antigen-specific ELISA and antigen affinity measurement.** ELISA plates were coated overnight with human IgG (Sanquin), insulin from bovine pancreas, actin from bovine muscle, lipopolysaccharide (LPS) from *Escherichia coli* O55:B5 (Sigma-Aldrich, Merck), and SSA/Ro52 or SSA/Ro60 (Diarect) in coating buffer (0.05M Na<sub>2</sub>CO<sub>3</sub>, 0.05M NaHCO<sub>3</sub>, pH 9.6). The ELISA

plates were incubated with recombinant lymphoma-derived IgM in serial dilutions starting from 1 μg/ml, and then subsequently incubated with horseradish peroxidase-conjugated mouse anti-human IgM (Southern Biotechnology), followed by development with tetramethylbenzidine as described previously (9,21).

Surface plasmon resonance assays were performed on an IBIS Mx96 instrument (IBIS Technologies) using a G-type anti-human IgM chip. Data on the binding affinity of the IgM antibodies were processed as described previously (22).

## RESULTS

***IGHV* and *IGLV* genes in salivary gland tissue from patients with SS-associated MALT lymphoma.** We studied a panel of 16 salivary gland samples from patients with SS-associated MALT lymphoma; 6 of the *IGHV* and *IGKV* sequences had been determined previously (9). Of 10 remaining new MALT lymphoma salivary gland samples, *IGHV* and *IGKV* transcripts were amplified by RT-PCR using *IGHV*- and *IGKV*-specific primers in combination with primers specific for the constant region of the μ heavy chain and κ light chain, respectively. All 10 MALT lymphoma samples expressed IgM antibodies, and their respective *IGHV* sequences were assessed (Table 1). In 1 of the samples (M93), we identified 2 distinct clonal *IGHV* sequences. In 8 of the 10 samples, we were able to identify the corresponding *IGKV*

sequences as well. Remarkably, 6 MALT lymphoma salivary gland samples expressed an *IGKV3-15* rearrangement, and 1 expressed an *IGKV3-20* rearrangement. *IGKV3-15* and *IGKV3-20* are typically found in *IGHV3-7*- and *IGHV1-69*-encoded stereotypic RFs, respectively (9). In the salivary gland samples from patients M87 and M88, the *IGKV* PCR yielded polyclonal amplicons, most likely attributable to a relatively low tumor load, and thus we were prohibited from reliably identifying the expressed *IGKV* sequences. All of the *IGHV* and *IGKV* genes identified were somatically mutated, except for the *IGKV* gene in the salivary gland tissue from patient M91, which was unmutated (Table 1 and Supplementary Figure 1, available on the *Arthritis & Rheumatology* web site at <http://online.library.wiley.com/doi/10.1002/art.41263/abstract>).

**Findings of VH-CDR3 amino acid sequence homology studies.** The VH-CDR3 aa sequences in the salivary glands from patients with MALT lymphoma were compared with the VH-CDR3 aa sequences from GenBank (release 228), obtained using the NCBI Protein-BLAST algorithm. According to our arbitrary criteria, the VH-CDR3s were considered homologous when they shared at least 60% aa sequence homology, with an allowed maximal gap of 3 aa. Except for samples M83, M91, M93-II, and M96, the VH-CDR3 aa sequences in all other samples showed VH-CDR3 homology with MALT lymphomas, but also with other B cell lymphomas such as CLL (see Supplementary Table 2, available on the *Arthritis & Rheumatology* web site at <http://online.library.wiley.com/doi/10.1002/art.41263/abstract>). The VH-CDR3s in salivary gland samples M88, M93-I, M94, and M95 were found to be homologous with those of B cells derived from inflamed salivary glands and, except for sample M95, all were also homologous with stereotypic RFs, i.e., VH-CDR3s in samples M93-I and M94 showed homology with stereotypic V3-7-RFs, and VH-CDR3

in sample M88 showed homology with stereotypic V1-69-RFs (Figure 1; see also Supplementary Tables 2 and 3, available on the *Arthritis & Rheumatology* web site at <http://onlinelibrary.wiley.com/doi/10.1002/art.41263/abstract>). Of note, sample M91 did not display a VH-CDR3 sequence that was homologous with stereotypic V1-69-RFs, although this salivary gland tissue sample expressed the canonical V1-69-RF gene combination of *IGHV1-69/IGHJ4* and *IGKV3-20*. Salivary gland sample M86 shared VH-CDR3 homology with an *IGHV3-30*-encoded HCV-associated MALT lymphoma (Figure 1).

#### Expression of monospecific RFs in most SS-associated MALT lymphoma salivary gland samples.

We produced, in total, 12 recombinant IgM antibodies from the MALT lymphoma salivary gland samples in our study, i.e., samples M86, M89, M91, M93-I, M94, and M96, and from 6 MALT lymphoma salivary gland samples from our earlier study, i.e., samples M5, M8, M11, M14, M21, and M22 (9). Of the salivary gland tissue from patient M93, we produced 2 recombinant IgM antibodies, M93-IA and M93-IB, which differed by 4 aa in *IGHV*. Of sample M96, we produced 2 recombinant IgM antibodies, M96-A and M96-B, which differed by 2 aa in the VH-CDR3 (see Supplementary Figure 1 [<http://online.library.wiley.com/doi/10.1002/art.41263/abstract>]).

The IgM antibodies produced from the MALT lymphoma samples were tested by ELISA for binding to insulin, actin, LPS, human IgG, SSA/Ro52, and SSA/Ro60. Except for samples M89, M8, and M14 in our earlier study, the IgM antibodies from all other MALT lymphoma salivary gland samples reacted with IgG and did not bind to any of the other antigens. The IgM antibodies from samples M91 and M96-B showed the strongest IgG-Fc binding (Figures 2A and B). It was noted that the M96-A IgM antibody showed a much weaker binding to IgG-Fc than the M96-B IgM antibody.

	IGHV	VH-CDR3 region	Homology	Genbank
<b>M86</b>	V3-30/JH4	C AQQAFSNK <b>WY-SIGDY</b> WGQG	60%	
<b>MALT-L of HCV patient</b>	V3-30/JH4	C AQQGFST <b>SWYVPTGGY</b> WGQG		<b>AAG33842</b>
<b>M88</b>	V1-69/JH4	C AREGKASVANGA <b>FDY</b> WGQG	67%	
<b>V1-69-RF, MR16-RF</b>	V1-69/JH4	C AREGKAGDYNNP <b>FDY</b> WGQG		<b>CAA84386</b>
<b>M93-IB</b>	V3-7/JH3	C ARGDYYDSSG <b>SNYHDAFDV</b> WGQG	89%	
<b>V3-7-RF, TT5-RF</b>	V3-7/JH3	C ARGDYYDSSG <b>-NYHDAFDV</b> WGQG		<b>AAB58444</b>
<b>M94</b>	V3-7/JH3	C ARGDYYDSSG <b>YIDAFDI</b> WGQG	94%	
<b>V3-7-RF, MALT-L M6</b>	V3-7/JH3	C ARGD <b>YFDSSGSFIDAFDI</b> WGQG		<b>AAP34731</b>
<b>M95</b>	V3-48/JH3	C AREPYS <b>DSSSFFP</b> GSFDI WGQG	61%	
<b>V3-7-RF, HCV MC-II</b>	V3-7/JH3	C ARGDYYDSSG <b>YHDAFDI</b> WGQG		<b>ACX46918</b>

**Figure 1.** VH-third complementarity-determining region (CDR3) amino acid sequence homology of salivary gland mucosa-associated lymphoid tissue (MALT)-type lymphomas of patients M86, M88, M93-IB, M94, and M95 with 4 stereotypic rheumatoid factors (RFs) and with a MALT lymphoma (MALT-L) from a hepatitis C virus (HCV)-infected patient. VH-CDR3 homology is calculated as a percentage of identical (red) and similar (blue) amino acids.

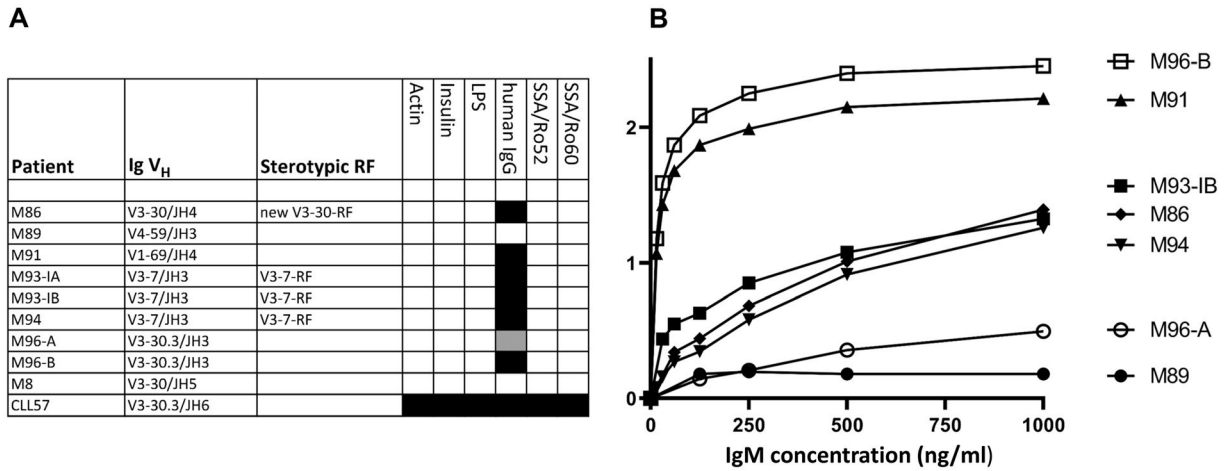


**Figure 2.** MALT lymphoma IgM antibodies characterized as high-affinity monoreactive RFs. In enzyme-linked immunosorbent assays (ELISAs), IgM derived from MALT lymphoma salivary gland samples M86, M91, M93-I, M94, and M96 show specific binding to coated human IgG (A), with different binding affinities (B). Values on the y-axis are the absorbance measured at 450 nm. Sample M8 is an IgM from a patient with Sjögren’s syndrome-associated MALT lymphoma who was analyzed previously and does not show RF activity. Sample CLL57 is an *IGV*-gene-unmutated IgM derived from a patient with B cell chronic lymphocytic leukemia (CLL) and shows strong polyreactivity. Black boxes indicate positive ELISA results at all IgM concentrations tested; the gray-shaded box indicates positive ELISA results at the 2 highest IgM concentrations tested. The IgMs were tested in at least 4 concentrations, i.e., 125, 250, 500, and 1,000 ng/ml. LPS = lipopolysaccharide (see Figure 1 for other definitions).

Overall, among our panel of 12 salivary gland MALT lymphoma IgM antibodies, 9 (75%) showed strong monoreactive RF activity. This panel included 5 stereotypic RFs, i.e., 1 V1-69-RF (sample M11), 3 V3-7-RFs (samples M5, M93-I, and M94), and the newly recognized *IGHV3-30*-encoded RF (sample M86).

**Recurrent replacement mutations in the *IGHV1-69* and *IGHV3-7* encoded salivary gland MALT lymphoma RFs.** We aligned the aa sequences of the *IGHV1-69*- and *IGHV3-7*-encoded salivary gland MALT lymphoma RFs, including 3 *IGHV1-69*-encoded RFs (samples M9, M11, and M22) and 2 *IGHV3-7*-encoded RFs (samples M5 and

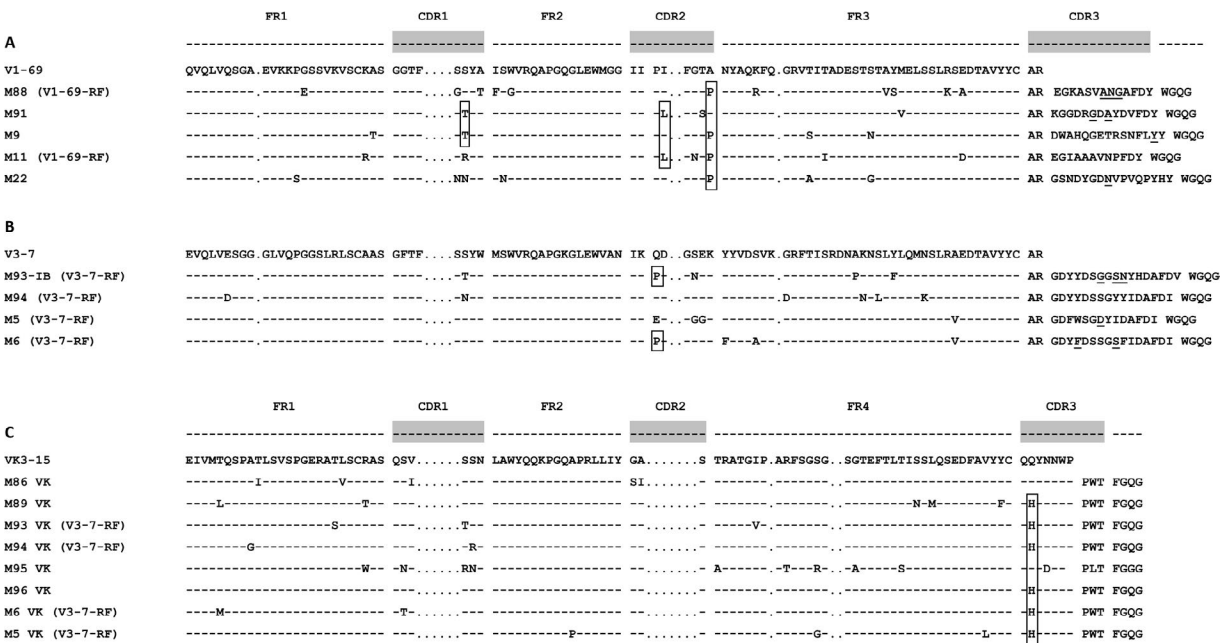


**Figure 3.** Alignment of amino acid sequences of *IGHV1-69*-, *IGHV3-7*-, and *IGKV3-15*- encoded RFs of salivary gland MALT lymphomas. Boxes highlight shared somatic replacement mutations, i.e., S36T in the VH-CDR1 of samples M91 and M9, I59L in the VH-CDR2 of samples M91 and M11, and A65P in the VH-CDR2 of samples M88, M9, M11, and M22 (A), Q58P in the VH-CDR2 of samples M93IB and M6 (B), and Q106H in the VK-CDR3 of samples M89, M93, M94, M96, M6, and M5 (C). Somatic replacement mutations in the VH-CDR3 are underlined. FR1 = framework region 1 (see Figure 1 for other definitions).

M6) from our earlier study (9). Our results demonstrated that the *IGHV1-69*-encoded RFs shared an A65P mutation (samples M88, M9, M11, and M22) or an I59L mutation (samples M91 and M11) in the VH-CDR2, while an S36T mutation in the VH-CDR1 was seen in 2 samples (M91 and M9). In the *IGHV3-7*-encoded RFs, we found a Q58P mutation that was shared between salivary gland samples M93-I and M6 only. Of note, samples M6 and M9 were from a patient with gastric MALT lymphoma and a patient with tonsillar MALT lymphoma (9).

Alignment of 8 *IGKV3-15* aa sequences, including *IGKV3-15* sequences of 2 stereotypic V3-7-RF-expressing MALT lymphoma salivary gland tissue samples from our previous study, demonstrated that all stereotypic V3-7-RFs (in samples M93, M94, M5, and M6) possessed a Q106H mutation in their VK-CDR3 region. In addition, an *IGHV4-59*-expressing MALT lymphoma (sample M89), which did not show RF activity, and an *IGHV3-30.3*-expressing RF (sample M96) also shared this Q106H mutation (Figures 3A–C).

**Contribution of somatic mutations to the affinities of the MALT lymphoma RFs.** We produced recombinant variants of the IgM antibodies of MALT lymphoma salivary gland samples M91, M93-I, M94, and M96, in which somatic mutations in *IGHV* and/or *IGKV* were reverted to their respective germline

configuration. Subsequently, we measured their affinity for IgG using surface plasmon resonance.

Reversion of the 4 replacement mutations in *IGHV* in MALT lymphoma salivary gland sample M91 had little effect on RF affinity (Figures 4A and B; compare the findings between bar A and bar B). However, when 2 replacement mutations in the VH-CDR3 (Figure 3) were also reverted, the RF affinity was completely lost (Figures 4A and B; compare the findings of bars A and B with bar C).

The 2 native stereotypic V3-7-RF variants of sample M93-I (variants M93-IA and M93-IB), which had 4 dissimilar aa in their *IGHV* sequences, had the same affinity for IgG-Fc (Figures 4A and B; compare the findings in bar D with bar E). All IgM variants in sample M93-I in which *IGHV*, with or without the VH-CDR3 and with or without *IGKV*, were reverted to germline configuration showed slightly higher affinities for IgG-Fc when compared to the natural IgM antibodies in sample M93-I (M93-IA and M93-IB) (Figures 4A and B; compare the findings in bars F, G, H, I, J, K, and L with bars D and E). Even a completely reverted IgM of M93-I, in which the H106Q mutation in VK-CDR3 was also reverted, showed an affinity that was similar to that of the naturally mutated M93-IA and M93-IB antibodies (Figures 4A and B; compare bar M with bars D and E). The 106-H mutation in the VK-CDR3, however, proved to be as important for RF affinity, as was illustrated by the 3 variant pairs (H and I, J and K, and L and M in Figures 4A and B), which showed higher RF affinities in the mutated 106-H

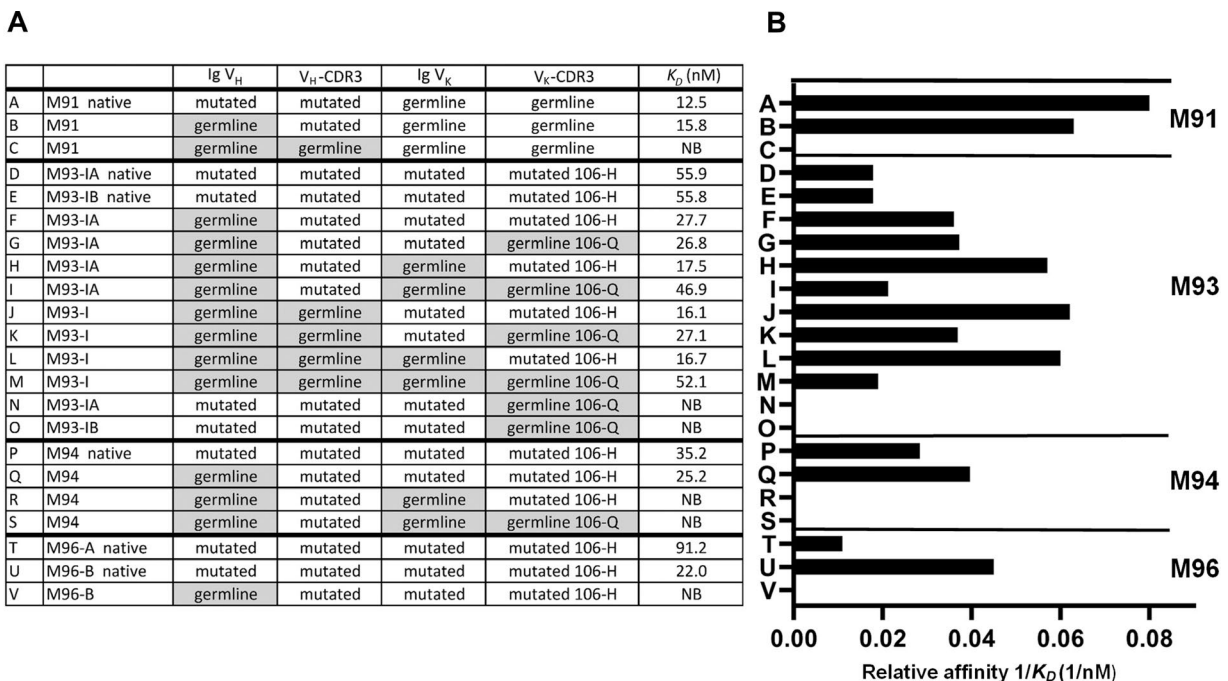


**Figure 4.** Binding affinities of MALT lymphoma RFs and germline-reverted variants for human IgG, as measured by surface plasmon resonance assay. **A**, *IGHV* and *IGKV* configurations for the native lymphoma RFs and germline-reverted variants of lymphoma RFs, are shown, along with their binding constants ( $K_D$ ) to indicate affinity for human IgG. **B**, Histograms display the  $1/K_D$  values of the native and germline-reverted variants of lymphoma RFs. Each letter to the left of the bars for each sample represents an individual recombinantly produced IgM antibody. NB = no binding; 106-H = histidine mutation on position 106 of VK-CDR3; 106-Q = germline glutamine on position 106 of VK-CDR3 (see Figure 1 for other definitions).

than in the 106-Q germline configuration. Most exemplary in this respect is the complete loss of RF affinity of M93-IA and M93-IB when the naturally mutated IgM antibodies were expressed with *IGKV*, in which only 106-Q was in germline configuration (Figures 4A and B; compare bars N and O).

The V3-7-RF-expressing IgM antibodies in salivary gland sample M94, in which the 6 replacement mutations in *IGHV* were reverted, displayed a slightly higher RF activity as compared to its native mutated variant. However, when the 2 replacement mutations in *IGKV* were also reverted, the RF activity was completely lost, which was already the case when the 106-H mutation was preserved (Figures 4A and B; compare bar R and bar S).

Finally, of the natural variants in salivary gland sample M96, the M96-B variant, which expressed dissimilar aa at 2 positions in the VH-CDR3 as compared to variant M96-A, showed a much higher affinity for IgG-Fc. Reversion of the 12 replacement mutations in *IGHV* in the M96-B variant resulted in the complete loss of RF activity (Figures 4A and B; compare bars T and U with bar V). Of note, the affinity measurements in MALT lymphoma salivary gland variants M96-A and M96-B correlated nicely with the results of the RF ELISA (as shown in Figure 2).

## DISCUSSION

The results of this study demonstrate that in most, but not all, MALT lymphomas occurring in patients with SS, BCRs with strong RF reactivity are expressed. Taken together with the results of a previous study by Martin et al (18) on 2 SS-associated MALT lymphomas, a total of 14 IgM antibodies of patients with SS-associated salivary gland MALT lymphoma have been produced recombinantly, of which 11 showed RF specificity. Five of these were stereotypic RFs, i.e., 1 sample with V1-69-RF, 3 samples with V3-7-RFs, and 1 sample (M86) that shared VH-CDR3 homology with an *IGHV3-30*-encoded HCV-associated MALT lymphoma, which could be considered as a newly identified stereotypic RF-BCR group.

Remarkably, all MALT lymphoma IgM antibodies that showed RF activity expressed an Igk light chain that was encoded either by *IGKV3-15* (samples M5, M86, M93-I, M94, and M96) or by *IGKV3-20* (samples M11, M21, M22, and M91). Of the 3 MALT lymphoma IgM antibodies without RF activity (samples M8, M14, and M89), only those in the salivary gland tissue of patient M89 expressed an *IGKV3-15*-encoded Igk. In 5 MALT lymphoma samples, we did not produce IgM antibodies but we garnered information about their *IGHV* sequences with or without *IGKV* (samples M83, M87, M88, M93-II, and M95); sample M95 also co-expressed *IGKV3-15* and an *IGHV3-48*-encoded Ig heavy chain with VH-CDR3 homology with stereotypic V3-7-RFs. Sample M83 expressed an *IGHV3-74*-encoded Ig heavy chain. *IGHV3-74* was also recently identified, by mass spectrometric sequencing of serum RFs, as one of the *IGHV* aa sequences present in 9 of 15 patients with SS (23). Finally, sample M88

expressed a stereotypic V1-69-RF Ig heavy chain. These data indicate that the MALT lymphoma salivary gland IgM antibodies in samples M83, M88, and M95 are likely also RFs.

Stereotypic RF reactivity is not unique to salivary gland MALT lymphomas. We have also demonstrated stereotypic RF reactivity in 2 samples from patients with gastric MALT lymphoma (9), 2 with CLL (12,15), and 4 with HCV-related B cell lymphoma (10). It is remarkable that whereas most SS-associated salivary gland MALT lymphomas express RFs, the frequency of stereotypic RF B cells in inflamed salivary glands of SS patients was found to be low (24,25). This suggests that RF B cells in SS, once recruited in an inflamed salivary gland and activated by IgG immune complexes, e.g., IgG-SSA/SSB, have a growth advantage and are prone to transform (25).

Analysis of *IGHV1-69*-encoded RFs demonstrated a limited number of recurrent replacement mutations, i.e., A65P and I59L in the VH-CDR2, and S36T in the VH-CDR1, which were present in 4 RFs, 2 RFs, and 2 RFs, respectively (of a total of 5). Among the 14 reported SS-associated MALT lymphoma-derived *IGHV1-69* sequences, whose RF activity was not explored in vitro, the A65P mutation was not found, whereas I59L was found in 2 cases and S36T was found in 3 cases (26,27). In the 11 *IGHV1-69*-encoded RFs found in HCV-infected patients with cryoglobulinemia, A65P was present in 3 cases, and both I59L and S36T were found in 2 cases (28).

In 2 of 4 stereotypic V3-7-RFs, we identified a recurrent Q58P mutation in the VH-CDR2. In the literature, Q58P was reported to be present in 2 of 4 *IGHV3-7* sequences in the salivary glands of patients with SS-associated MALT lymphoma (26,27). Alignment of the corresponding *IGKV3-15* aa sequences of our stereotypic V3-7-RFs showed that all 4 carried a Q106H replacement mutation in their VK-CDR3 region. Interestingly, the *IGHV4-59*-expressing salivary gland MALT lymphoma from patient M89, which did not display RF activity, and the *IGHV3-30.3*-expressing RF from patient M96 both harbored a Q106H mutation in the VK-CDR3 as well. In the literature, it was reported that Q106H was found in an SS-associated MALT lymphoma (18) and in a stereotypic V3-7-RF from a patient with CLL (12). For both of these lymphomas, in vitro RF activity was demonstrated (12,18).

We observed that MALT lymphoma salivary gland sample M91 expressed the stereotypic combination of *IGHV1-69* and *IGKV3-20*. However, this RF does not share V<sub>H</sub>-CDR3 homology with stereotypic V1-69-RFs. Reversion of its 4 *IGHV* replacement mutations showed a small reduction in RF affinity, and when the 2 replacement mutations in the VH-CDR3 were also reverted, IgG binding was completely lost.

These results were recently clarified in a description of the crystal structure of an *IGHV1-69/IGKV3-20*-encoded RF (YES8c) in complex with IgG1-Fc (29). The YES8c RF also does not display VH-CDR3 homology with V1-69-RFs. The VH-CDR3 in sample M91 shared 47% aa sequence homology with the VH-CDR3 of YES8c. In total, atoms of 12 *IGHV* aa of YES8c were

shown to interact with the CH2 and CH3 regions of IgG1-Fc (Figure 5A). Alignment of the sequences in samples M91 and YES8c demonstrates that 7 of these 12 aa are shared between M91 and YES8c. In sample M91, only 2 of the 4 replacement mutations in the *IGHV* region (S36T and I59L) were contact residues with IgG-Fc, of which the I59L mutation, present both in M91 and in YES8c, led to a lower affinity in YES8c. Since serine and threonine are similar, the S36T mutation likely does not add much to the affinity in sample M91 (29). It thus is envisioned that the reversion of these 4 replacement mutations in sample M91 will yield a small difference in RF affinity (Figure 4). Interestingly, the R111.1-G mutation in the M91 VH-CDR3 resulted in an identical aa sequence as that in YES8c. The 111.1-G mutation was shown to interact with IgG1-Fc (Figure 5B). The contribution of a patch of 4 or 5 contiguous aa in the VH-CDR3 to the Fc-IgG1 binding affinity was substantiated by the complete loss of RF activity upon germline reversion of 2 mutations within this patch. Eight *IGKV* aa of YES8c, of which 7 aa are identical to those in M91, were shown to interact with IgG1-Fc (Figure 5A). Finally, the VH-CDR3 of YES8c shared 73% homology with the VH-CDR3 expressed by an SS-associated salivary gland MALT lymphoma from GenBank (sample T580B) (Figure 5B).

The results of the IgG binding studies of the 12 constructed variants of the RFs in MALT lymphoma salivary gland sample M93-I were, in part, more difficult to interpret. In sample M93-I, a completely germline-reverted *IGHV//IGKV* variant showed a similar RF affinity as that of the native IgM antibodies of M93-IA and IB. All reverted variants of *IGHV*, with or without the VH-CDR3 and with or without *IGKV*, displayed even slightly enhanced RF

affinities. However, the 106-H mutation of the VK-CDR3 contributed to the RF affinity, which was illustrated by the variant pairs that differed only with respect to each other between 106-H and 106-Q. Most explanatory in this respect is the complete loss of RF affinity when the naturally mutated IgM antibodies of M93-IA and IB were expressed with *IGKV*, in which only 106-Q was in germline configuration (Figures 4A and B, bar N and bar O). Unfortunately, of the stereotypic V3-7-RFs, no crystal structure has as yet been reproduced. Our observation that reversion of particular replacement mutations in RFs can lead to higher IgG-Fc affinities has been described before (28,29).

A completely germline-reverted *IGHV//IGKV* variant of V3-7-RF in sample M94 did not show any IgG binding. The VH-CDR3 of M96-A harbored 2 extra replacement mutations as compared to that of M96-B, and yet it showed a much lower affinity for IgG, indicating that the germline aa at this position are important for RF affinity. Moreover, reversion of 12 *IGHV* replacement mutations both in M96-A and in M96-B resulted in a complete loss of IgG binding.

Taken together, these findings indicate that somatic *IGV*-gene mutations contribute differently to the affinity of the RFs for IgG-Fc. Germline reversion of replacement mutations in *IGHV*, including the VH-CDR3 and, if applicable, also *IGKV*, resulted in lower RF affinities of the IgM antibodies of samples M91, M94, and M96. The affinities of the RFs varied, with binding constants ( $K_D$ ) ranging between 91 nM and 12 nM. These affinity values are lower than we have previously measured for tetanus toxoid-specific antibodies, which were found to have  $K_D$  values between 1.9 nM and 0.1 nM (22). Overall, the experiments showing

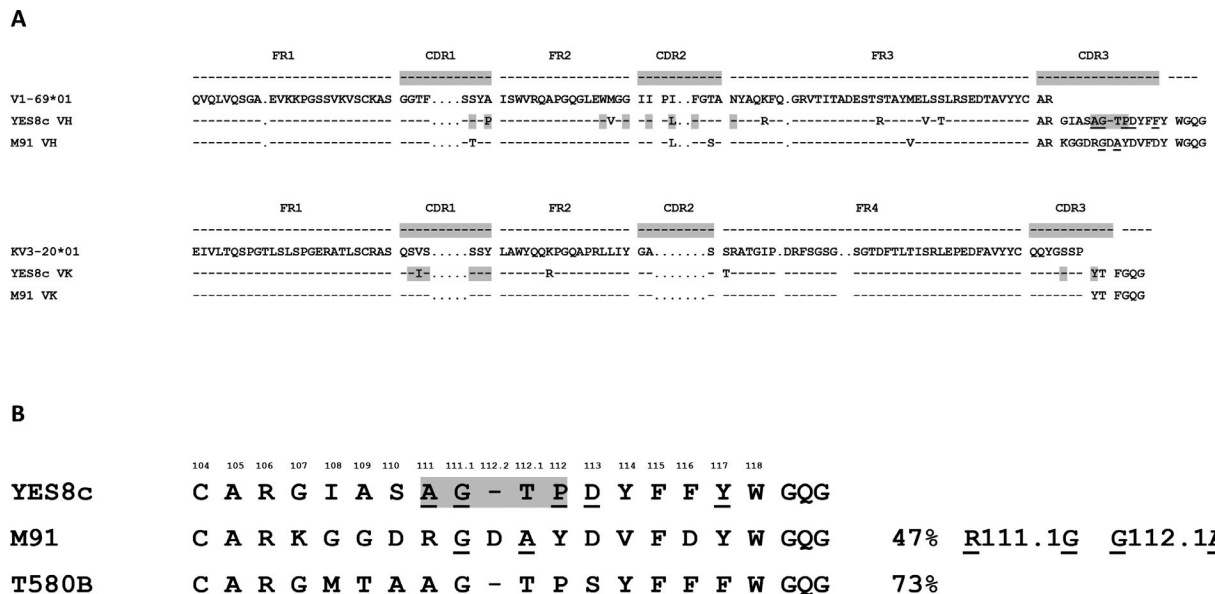


**Figure 5.** Alignment of the *IGHV1-69*-encoded RFs of YES8c and M91. **A**, Somatic replacement mutations, as compared with the *IGHV1-69* and *IGKV3-20* germline sequences, are indicated. **B**, Alignment of the VH-CDR3 amino acid sequences in YES8c, M91, and the homologous T580B, which originated from a patient with a Sjögren's syndrome-related MALT lymphoma, are indicated. Somatic replacement mutations are underlined. Gray-shaded boxes highlight the amino acids of RFs in YES8c that are the contact residues with IgG-Fc. FR1 = framework region 1 (see Figure 1 for other definitions).



reversion of *IGV*-gene mutations have demonstrated that the RFs are affinity-selected. Even the germline-converted RFs of M93-IA and IB, which displayed an affinity similar to its naturally mutated variant, indicated that although the *IGV*-gene mutations did not enhance the RF affinity, they still seemed to be selected to preserve the RF affinity and specificity.

Recently, it was shown that the RF epitopes of monomeric IgG in solution are shielded for soluble RFs and RF-expressing B cells. The RF epitopes may become accessible, e.g., after physical adsorption on a hydrophobic surface in ELISA plates, by heat treatment or in vivo by binding of IgG to its antigen-forming IgG immune complexes (30). The fact that RF B cells can be activated only by IgG in immune complexes was shown before (31,32). Moreover, in a mouse model, RF B cells were shown to be activated by IgG–chromatin complexes through the synergistic engagement of the RF-BCR and Toll-like receptor 9 (TLR-9) (33). As it is known that SSA/SSB are part of a ribonucleoprotein complex containing single-stranded RNA stem-loop structures, RF B cells in SS salivary glands may also be activated by IgG–SSA/SSB immune complexes via the RF-BCR and TLR-7. In support of this, it has recently been shown that IgG and IgA anti-SSA/Ro52, Ro60, and SSB/La48 are produced by ~30% of salivary gland plasmablasts in patients with SS, and the corresponding autoantibodies are found in the serum (34). Similarly, using biotin-labeled SSA/Ro60 in immunohistochemical analyses, we detected in situ anti-SSA/Ro60–specific autoantibodies, as well as plasma cells, producing anti-SSA/Ro60–specific autoantibodies in salivary gland samples from 3 patients with SS and in all 5 tested samples from patients with SS-associated MALT lymphoma (samples M14 and M93–M96) (see Supplementary Figure 2, available on the *Arthritis & Rheumatology* web site at <http://onlinelibrary.wiley.com/doi/10.1002/art.41263/abstract>).

Somatic mutations in *IGV* genes are classically introduced during T helper cell–dependent germinal center (GC) reactions. However, it is unlikely that T helper cells specific for IgG peptides would escape negative selection during their development. The most obvious pathway for RF B cells to receive T cell help is that autoantigens that are contained in IgG–immune complexes are internalized and delivered to major histocompatibility complex class II–processing compartments, leading to the presentation of peptides of autoantigens, e.g., of SSA/Ro52/Ro60 and SSB/La48 (35,36). The fact that highly somatically mutated IgG autoantibodies against SSA/Ro52, Ro60, and SSB/La48 proteins are frequently found in patients with SS and in patients with systemic lupus erythematosus indicates that these proteins can initiate a GC reaction, in which the autoreactive B cells receive cognate help from autoreactive T cells that recognize peptides of SSA/Ro52, Ro60, and SSB/La48 (34,37,38). These same T helper cells may thus also permit indirectly, and perhaps less efficiently, a GC reaction of RF B cells. Normally, a proportion of B cells that have acquired high-affinity BCRs undergo class switch recombination and become expressed as IgG. However, class-switched

RF B cells that express IgG will bind neighboring IgG molecules, which likely will result in overstimulation and autodeletion of these IgG-expressing RF B cells. Similarly, IgM-RF–expressing B cells in which the affinities are too high might become overstimulated by IgG bound to its antigen, and thereby become anergic or deleted. The possibility that chronic stimulation of RF B cells can lead to anergy has indeed been demonstrated in some patients with SS and patients with chronic HCV infection, whose peripheral blood harbored a population of expanded, unresponsive CD21<sup>-low</sup> RF B cells (39–41).

In conclusion, the majority of SS-associated salivary gland MALT lymphomas express BCRs with monoreactive, high-affinity RF activity. These RFs carry somatic mutations in their *IGV* genes and are affinity-selected for IgG binding. In patients with SS, we hypothesize that IgG–autoantigen complexes in inflamed salivary glands provide a growth advantage to RF-expressing B cells and are key in the pathogenesis of RF-expressing MALT lymphoma.

## AUTHOR CONTRIBUTIONS

All authors were involved in drafting the article or revising it critically for important intellectual content, and all authors approved the final version to be published. Dr. Bende had full access to all of the data in the study and takes responsibility for the integrity of the data and the accuracy of the data analysis.

**Study conception and design.** Bende, Janssen, Haacke, Kroese, Guikema, van Noesel.

**Acquisition of data.** Bende, Janssen, Beentjes, Wormhoudt, Wagner, Haacke.

**Analysis and interpretation of data.** Bende, Janssen, Beentjes, Wormhoudt, Wagner, Haacke, Kroese, Guikema, van Noesel.

## ADDITIONAL DISCLOSURES

Author Wagner is an employee of AIMM Therapeutics.

## REFERENCES

- Zucca E, Bertoni F. The spectrum of MALT lymphoma at different sites: biological and therapeutic relevance. *Blood* 2016;127:2082–92.
- Bende RJ, van Maldegem F, van Noesel CJ. Chronic inflammatory disease, lymphoid tissue neogenesis and extranodal marginal zone B-cell lymphomas. *Haematologica* 2009;94:1109–23.
- Nocturne G, Pontarini E, Bombardieri M, Mariette X. Lymphomas complicating primary Sjögren's syndrome: from autoimmunity to lymphoma. *Rheumatology (Oxford)* 2019. E-pub ahead of print.
- Goules AV, Tzioufas AG. Lymphomagenesis in Sjögren's syndrome: predictive biomarkers towards precision medicine. *Autoimmun Rev* 2019;18:137–43.
- Ekstrom-Smedby K, Vajdic CM, Falster M, Engels EA, Martinez-Maza O, Turner J, et al. Autoimmune disorders and risk of non-Hodgkin lymphoma subtypes: a pooled analysis within the InterLymph Consortium. *Blood* 2008;111:4029–38.
- Kroese FG, Abdulahad WH, Haacke E, Bos NA, Vissink A, Bootsma H. B-cell hyperactivity in primary Sjögren's syndrome [review]. *Expert Rev Clin Immunol* 2014;10:483–99.
- Pollard RP, Pijpe J, Bootsma H, Spijkervet FK, Kluijn PM, Roodenburg JL, et al. Treatment of mucosa-associated lymphoid tissue lymphoma in Sjögren's syndrome: a retrospective clinical study. *J Rheumatol* 2011;38:2198–208.

8. Nocturne G, Virone A, Wan-Fai Ng, Le Guern V, Hachulla E, Cornec D, et al. Rheumatoid factor and disease activity are independent predictors of lymphoma in primary Sjögren's syndrome. *Arthritis Rheumatol* 2016;68:977–85.
9. Bende RJ, Aarts WM, de Jong D, Pals ST, van Noesel CJ. Among B-cell non-Hodgkin's lymphomas, MALT lymphomas express a unique antibody repertoire with frequent rheumatoid factor reactivity. *J Exp Med* 2005;201:1229–41.
10. Bende RJ, Janssen J, Wormhoudt TA, Wagner K, Guikema JE, van Noesel CJ. Identification of a novel stereotypic IGHV4-59/IGHJ5-encoded B-cell receptor subset expressed by various B-cell lymphomas with high affinity rheumatoid factor activity. *Haematologica* 2016;101:e200–3.
11. Van Maldegem F, Wormhoudt TA, Mulder MM, Oud ME, Schilder-Tol E, Musler AR, et al. Chlamydia psittaci-negative ocular adnexal marginal zone B-cell lymphomas have biased VH4-34 immunoglobulin gene expression and proliferate in a distinct inflammatory environment. *Leukemia* 2012;26:1647–53.
12. Hoogeboom R, Wormhoudt TA, Schipperus MR, Langerak AW, Dunn-Walters DK, Guikema JE, et al. A novel chronic lymphocytic leukemia subset expressing mutated IGHV3-7-encoded rheumatoid factor B-cell receptors that are functionally proficient [letter]. *Leukemia* 2013;27:738–40.
13. Mariette X. Lymphomas complicating Sjögren's syndrome and hepatitis C virus infection may share a common pathogenesis: chronic stimulation of rheumatoid factor B cells. *Ann Rheum Dis* 2001;60:1007–10.
14. De Re V, De Vita S, Marzotto A, Rupolo M, Gloghini A, Pivetta B, et al. Sequence analysis of the immunoglobulin antigen receptor of hepatitis C virus-associated non-Hodgkin lymphomas suggests that the malignant cells are derived from the rheumatoid factor-producing cells that occur mainly in type II cryoglobulinemia. *Blood* 2000;96:3578–84.
15. Kostareli E, Gounari M, Janus A, Murray F, Brochet X, Giudicelli V, et al. Antigen receptor stereotypy across B-cell lymphoproliferations: the case of IGHV4-59/IGKV3-20 receptors with rheumatoid factor activity [letter]. *Leukemia* 2012;26:1127–31.
16. Charles ED, Green RM, Marukian S, Talal AH, Lake-Bakaar GV, Jacobson IM, et al. Clonal expansion of immunoglobulin M+CD27+ B cells in HCV-associated mixed cryoglobulinemia. *Blood* 2008;111:1344–56.
17. Borretzen M, Chapman C, Natvig JB, Thompson KM. Differences in mutational patterns between rheumatoid factors in health and disease are related to variable heavy chain family and germ-line gene usage. *Eur J Immunol* 1997;27:735–41.
18. Martin T, Weber JC, Levallois H, Labouret N, Soley A, Koenig S, et al. Salivary gland lymphomas in patients with Sjögren's syndrome may frequently develop from rheumatoid factor B cells. *Arthritis Rheum* 2000;43:908–16.
19. Van Dongen JJ, Langerak AW, Bruggemann M, Evans PA, Hummel M, Lavender FL, et al. Design and standardization of PCR primers and protocols for detection of clonal immunoglobulin and T-cell receptor gene recombinations in suspect lymphoproliferations: report of the BIOMED-2 Concerted Action BMH4-CT98-3936. *Leukemia* 2003;17:2257–317.
20. Brochet X, Lefranc MP, Giudicelli V. IGHV/QUEST: the highly customized and integrated system for IG and TR standardized V-J and V-D-J sequence analysis. *Nucleic Acids Res* 2008;36:W503–8.
21. Bende RJ, Jochems GJ, Frame TH, Klein MR, van Eijk RV, van Lier RA, et al. Effects of IL-4, IL-5 and IL-6 on growth and immunoglobulin production of Epstein-Barr virus-infected human B cells. *Cell Immunol* 1992;143:310–23.
22. Slot LM, Wormhoudt TA, Kwakkenbos MJ, Wagner K, Ballering A, Jongejan A, et al. De novo gene mutations in normal human memory B cells. *Leukemia* 2019;33:1219–30.
23. Wang JJ, Reed JH, Colella AD, Russell AJ, Murray-Brown W, Chataway TK, et al. Molecular profiling and clonal tracking of secreted rheumatoid factors in primary Sjögren's syndrome. *Arthritis Rheumatol* 2018;70:1617–25.
24. Visser A, Doorenspleet ME, de Vries N, Spijkervet FK, Vissink A, Bende RJ, et al. Acquisition of N-glycosylation sites in immunoglobulin heavy chain genes during local expansion in parotid salivary glands of primary Sjögren patients. *Front Immunol* 2018;9:491.
25. Bende RJ, Slot LM, Hoogeboom R, Wormhoudt TA, Adeoye AO, Guikema JE, et al. Stereotypic rheumatoid factors that are frequently expressed in mucosa-associated lymphoid tissue-type lymphomas are rare in the labial salivary glands of patients with Sjögren's syndrome. *Arthritis Rheumatol* 2015;67:1074–83.
26. Bahler DW, Swerdlow SH. Clonal salivary gland infiltrates associated with myoepithelial sialoadenitis (Sjögren's syndrome) begin as nonmalignant antigen-selected expansions. *Blood* 1998;91:1864–72.
27. Miklos JA, Swerdlow SH, Bahler DW. Salivary gland mucosa-associated lymphoid tissue lymphoma immunoglobulin V(H) genes show frequent use of V1-69 with distinctive CDR3 features. *Blood* 2000;95:3878–84.
28. Charles ED, Orloff MI, Nishiuchi E, Marukian S, Rice CM, Dustin LB. Somatic hypermutations confer rheumatoid factor activity in hepatitis C virus-associated mixed cryoglobulinemia. *Arthritis Rheum* 2013;65:2430–40.
29. Shiroishi M, Ito Y, Shimokawa K, Lee JM, Kusakabe T, Ueda T. Structure-function analyses of a stereotypic rheumatoid factor unravel the structural basis for germline-encoded antibody autoreactivity. *J Biol Chem* 2018;293:7008–16.
30. Maibom-Thomsen SL, Trier NH, Holm BE, Hansen KB, Rasmussen MI, Chailyan A, et al. Immunoglobulin G structure and rheumatoid factor epitopes. *PLoS One* 2019;14:e0217624.
31. Herlands RA, William J, Hershberg U, Shlomchik MJ. Anti-chromatin antibodies drive in vivo antigen-specific activation and somatic hypermutation of rheumatoid factor B cells at extrafollicular sites. *Eur J Immunol* 2007;37:3339–51.
32. Avalos AM, Busconi L, Marshak-Rothstein A. Regulation of autoreactive B cell responses to endogenous TLR ligands. *Autoimmunity* 2010;43:76–83.
33. Leadbetter EA, Rifkin IR, Hohlbaum AM, Beaudette BC, Shlomchik MJ, Marshak-Rothstein A. Chromatin-IgG complexes activate B cells by dual engagement of IgM and Toll-like receptors. *Nature* 2002;416:603–7.
34. Takeshita M, Suzuki K, Kaneda Y, Yamane H, Ikeura K, Sato H, et al. Antigen-driven selection of antibodies against SSA, SSB and the centromere 'complex', including a novel antigen, MIS12 complex, in human salivary glands. *Ann Rheum Dis* 2019;79:150–8.
35. Shlomchik MJ. Sites and stages of autoreactive B cell activation and regulation. *Immunity* 2008;28:18–28.
36. Roosnek E, Lanzavecchia A. Efficient and selective presentation of antigen-antibody complexes by rheumatoid factor B cells. *J Exp Med* 1991;173:487–9.
37. Mietzner B, Tsuji M, Scheid J, Velinzon K, Tiller T, Abraham K, et al. Autoreactive IgG memory antibodies in patients with systemic lupus erythematosus arise from nonreactive and polyreactive precursors. *Proc Natl Acad Sci U S A* 2008;105:9727–32.
38. Reed JH, Gorny MK, Li L, Cardozo T, Buyon JP, Clancy RM. Ro52 autoantibodies arise from self-reactive progenitors in a mother of a child with neonatal lupus. *J Autoimmun* 2017;79:99–104.
39. Charles ED, Brunetti C, Marukian S, Ritola KD, Talal AH, Marks K, et al. Clonal B cells in patients with hepatitis C virus-associated mixed cryoglobulinemia contain an expanded anergic CD21low B-cell subset. *Blood* 2011;117:5425–37.

40. Glauzy S, Boccitto M, Bannock JM, Delmotte FR, Saadoun D, Cacoub P, et al. Accumulation of antigen-driven lymphoproliferations in complement receptor 2/CD21<sup>-/low</sup> B cells from patients with Sjögren's syndrome. *Arthritis Rheumatol* 2018;70:298–307.
41. Bende RJ, van Noesel CJ. Rheumatoid factor reactivity of expanded CD21<sup>-/low</sup> B cells in patients with Sjögren's syndrome: comment on the article by Glauzy et al [letter]. *Arthritis Rheumatol* 2019;71:169–70.